The EMBO Journal Vol.17 No.17 pp.5238–5248, 1998

Crystal structure of the complex formed by the membrane type 1-matrix metalloproteinase with the tissue inhibitor of metalloproteinases-2, the soluble progelatinase A receptor

Carlos Fernandez-Catalan, Wolfram Bode[1], Robert Huber, Dusan Turk[2], Juan J.Calvete[3], Andrea Lichte[4], Harald Tschesche[4] and Klaus Maskos

Max-Planck-Institut für Biochemie, Am Klopferspitz 18a, D-82152 Martinsried-Planegg, [3]Institut für Reproduktionsmedizin, Tierärztliche Hochschule Hannover, Bunteweg 15, D-30559 Hannover, [4]Universität Bielefeld, Abteilung Biochemie I, Universitätsstraβe 25, D-33615 Bielefeld, Germany and [2]Department of Biochemistry and Molecular Biology, Jozef Stefan Institute, Jamova 39, SL-61111 Ljubljana, Slovenia

[1]Corresponding author
e-mail: bode@biochem.mpg.de

The proteolytic activity of matrix metalloproteinases (MMPs) towards extracellular matrix components is held in check by the tissue inhibitors of metalloproteinases (TIMPs). The binary complex of TIMP-2 and membrane-type-1 MMP (MT1-MMP) forms a cell surface located 'receptor' involved in pro-MMP-2 activation. We have solved the 2.75 Å crystal structure of the complex between the catalytic domain of human MT1-MMP (cdMT1-MMP) and bovine TIMP-2. In comparison with our previously determined MMP-3–TIMP-1 complex, both proteins are considerably tilted to one another and show new features. CdMT1-MMP, apart from exhibiting the classical MMP fold, displays two large insertions remote from the active-site cleft that might be important for interaction with macromolecular substrates. The TIMP-2 polypeptide chain, as in TIMP-1, folds into a continuous wedge; the A-B edge loop is much more elongated and tilted, however, wrapping around the S-loop and the β-sheet rim of the MT1-MMP. In addition, both C-terminal edge loops make more interactions with the target enzyme. The C-terminal acidic tail of TIMP-2 is disordered but might adopt a defined structure upon binding to pro-MMP-2; the Ser2 side-chain of TIMP-2 extends into the voluminous S1′ specificity pocket of cdMT1-MMP, with its Oγ pointing towards the carboxylate of the catalytic Glu240. The lower affinity of TIMP-1 for MT1-MMP compared with TIMP-2 might be explained by a reduced number of favourable interactions.

Keywords: crystal structure/matrix metalloproteinase/progelatinase A activator/proteinase complex/tissue inhibitor of metalloproteinases

Introduction

Matrix metalloproteinases (MMPs, matrixins) form a family of zinc endopeptidases implicated in connective tissue remodelling (Woessner, 1991; Nagase, 1997). These MMPs have been subgrouped, according to their structural and functional properties, into the collagenases, gelatinases, stromelysins and matrilysin/elastase (together making up the 'classical' MMPs), and the membrane-type MMPs (MT-MMPs). MMPs are synthesized as pro-proteinases consisting of an N-terminal propeptide followed by the catalytic domain (cd), which in turn (except for matrilysin) is linked to a C-terminal haemopexin-like domain.

The most recently detected MT-MMPs (Sato *et al*., 1994), which presently comprise three closely related (MT1-, MT2- and MT3-MMP, see Figure 4) and one more diverse species (MT4-MMP), exhibit considerable differences to the classical MMPs; they possess a C-terminal extension including a trans-membrane domain, have a different activation cleavage site, and show unique sequence features in their catalytic domain (Sato *et al*., 1994). ProMT1-MMP is expressed in various tissues including carcinoma and/or tumour stroma cells (Okada *et al*., 1995; Takino *et al*., 1995). It has been shown to be processed at Arg111-Tyr112 by furin-like convertases, and localized as the mature MT1-MMP on cell surfaces (Pei and Weiss, 1996; Sato *et al*., 1996). MT1-MMP is capable of proteolyzing extracellular matrix proteins such as gelatin, fibronectin, proteoglycans, aggrecan and collagens of type I, II and III (Pei and Weiss, 1996; Ohuchi *et al*., 1997; d'Ortho *et al*., 1997). Soluble proMT1-MMP seems to possess some autoactivating properties, giving rise to MT1-MMP species starting with Ala113 (Sato *et al*., 1996) or Ile114 (Lichte *et al*., 1996).

Virtually all MMPs form tight 1:1 complexes with the tissue inhibitors of metalloproteinases (TIMPs) (see references in Murphy and Willenbrock, 1995), which currently comprise four different species (TIMPs-1 to -4) exhibiting 41–52% sequence identity (see Figure 5). This inhibition is not particularly selective; the only exception known to date is the rather weak interaction of TIMP-1 with MT1-MMP (Sato *et al*., 1996; Will *et al*., 1996). The TIMPs are multifunctional proteins, with other functions such as growth factor-like activity or inhibition of angiogenesis (see references in Gomez *et al*., 1997; Cawston, 1998). All TIMP-2 species known so far (of bovine, human, mouse and rat origin) exhibit 194 residues, are non-glycosylated, and possess an elongated negatively charged tail (Stetler-Stevenson *et al*., 1989; Boone *et al*., 1990). TIMP-2 is unique in that it can also bind to the pro-form of gelatinase A (pro-MMP-2), presumably via secondary exosites on both C-terminal domains (Kolkenbrock *et al*., 1991; Murphy *et al*., 1992; Fridman *et al*., 1992). The TIMP-2 complex with MT1-MMP acts as a cell surface-bound 'receptor' involved in the processing of progelatinase A (Strongin *et al*., 1993, 1995; Kinoshita *et al*., 1996; Will *et al*., 1996); the activated gelatinase A is believed to be crucial for various remodelling processes, but also for chronic degenerative


A
sII
sI
hA
sIII
sV
sIV
hB
hC
sA
sB
sE
sG
sC
sD
hI
sH
hIII
hIV
sF
sI
sJ
hII


B

diseases, and tumour invasion and metastasis, rendering MT1-MMP an early player in the tumour scenario and thus an interesting target for tumour therapy.

Our recently published crystal structure of the MMP-3–TIMP-1 complex (Gomis-Rüth *et al*., 1997) revealed the principal mechanism of TIMP inhibition and the general interaction geometry between MMPs and TIMPs, and for the first time showed the complete fold of a TIMP inhibitor. Of TIMP-2, only a preliminary NMR structure of its N-terminal part has been published so far (Williamson *et al*., 1994, 1997), and no crystal structure of an MT-MMP (fragment) is known to date. We have now crystallized the complex formed between the recombinant catalytic domain of MT1-MMP (cdMT1-MMP) and full-length TIMP-2 derived from bovine seminal plasma (BSP; Calvete *et al*., 1996), and have determined its X-ray crystal structure. This crystallographic cdMT1-MMP–TIMP-2 structure allows us to identify the structural determinants of each individual protein component and their interactions, but simultaneously shows the key features of the membrane receptor thought to play an important role in progelatinase A activation.

Results

Overall structure

In the cdMT1-MMP–TIMP-2 complex, the elongated wedge-shaped TIMP-2 inhibitor slots into the active-site cleft of the catalytic domain of MT1-MMP (Figure 1A). The solvent-accessible surface of each component is reduced in the complex by ~1250 Å^2. In general, this complex looks similar to that of our previous MMP-3–TIMP-1 complex (Gomis-Rüth *et al*., 1997) (Figure 1B). Noteworthy differences are a much more elongated sA–sB loop of TIMP-2 grabbing toward the surface of the MMP β-sheet, and an adjacent MT-characteristic insertion loop of cdMT1-MMP protruding from this surface (for nomenclature, see Figure 1A). A detailed comparison not only shows that each structural component has a number of unique features (see below), but also that proteinase and inhibitor are arranged differently; if both MMP components are optimally superimposed, both inhibitors are tilted according to rotations of ~20, 10 and 5° about SerI4 (with the prefix I indicating inhibitor residues) around a vertical, a perpendicular and a horizontal axis (Figure 1B).

The MT1-MMP catalytic domain

Like the classical MMPs, the cdMT1-MMP is a spherical molecule notched at its periphery to give a short active-site cleft, which separates a small 'lower' subdomain from the 'upper' main molecular body. As in the other MMPs, this larger part essentially consists of a highly twisted five-stranded mixed β-pleated sheet, flanked by three surface loops on its convex side and by two α-helices on its concave side. The polypeptide chain starts on the molecular surface (on the left hand side of Figure 1A) visible from its first residue (Ile114) onwards, passes β-strand sI, helix hA, β-strands sII, sIII, sIV and sV, until entering the 'active-site helix' hB (for the extension of these secondary structure elements see Figure 4). The spur-like MT-MMP-specific loop (see below) bridges sI to connect the peripheral strand sII with the central strand sIII, which is linked with sIV via an 'S-shaped double loop' followed by the cleft-sided 'bulge' strand which continues into the antiparallel 'edge' strand sIV. The chain then loops over to sV, which is connected through a large open loop with hB, which in turn provides the 'catalytic' Glu240 and two (His239 and 243) of the three imidazol ligands of the 'catalytic zinc' ZN001 (Figure 3).

This active-site helix, hB, stops abruptly at Gly246 where the chain bends down, runs (under provision of the third zinc ligand, His249) through a wide spiral terminating in the 1,4-tight 'Met-turn' Ala-Ile-Met257-Ala (Bode *et al*., 1994) (Figure 1A). The chain then turns back to the molecular surface to segment Pro259-Phe260-Tyr261 (forming the outer wall of the S1′ pocket, Figures 2B and 3), and runs through another wide loop before it passes the C-terminal α-helix C, which ends at Tyr283-Gly284. The following linker segment deviating from the molecular surface is partially defined up to Ser287, before it fully disappears in the bulk water.

The active-site cleft of cdMT1-MMP (see Figure 2) has a shape similar to that of the classical MMPs. Bounded at the upper rim by the bulge-edge segment, and at the lower side by His249 and the S1′ wall-forming segment, it is relatively flat to the left (non-primed subsites), but carves into the molecular surface at the catalytic zinc and to the right side (primed subsites). To the right of the catalytic zinc (Figure 2) lies the S1′ pocket, which is very similar in size and lining to that of MMP-3; it likewise extends to the opposite surface of the domain more resembling a continuous pore, and is well suited to accommodate quite elongated P1′ side chains (Mucha *et al*., 1998). Further to the right, another pocket opens which could provide a specific S3′ subsite. Noteworthy is the Phe260 benzyl side chain of the wall-forming segment, which extends away from the molecule; this Phe residue is conserved among MT1-, MT2- and MT3-MMP and stromelysin-3, but is replaced by medium-sized and/or more polar residues in the classical MMPs.

cdMT1-MMP contains four highly occupied metal sites binding two zinc and two calcium ions (Figure 1) in a similar manner to the classical MMPs, but lacks a third calcium binding site. The catalytic zinc ZN001 resides in the central part of the active-site cleft liganded by the imidazoyl Nε2 nitrogens of His239, His243 and His 249, and CysI1 N and O of the inhibitor (see below and Figure 3). The second 'structural zinc', ZN002, is packed between the first loop of the S-shaped double loop and the β-sheet surface, surrounded in a tetrahedral manner by the imidazoyl Nε2 nitrogens of His186 (S-loop) and His201 (sIV), the Nδ1 nitrogen of His214 (sV), and one carboxylate oxygen of Asp188 (S-loop), with the S-loop

Fig. 1. Front view ribbon of the MMP–TIMP complexes. Figures drawn with SETOR (Evans, 1993). (**A**) Complex formed between cdMT1-MMP (top, gold) and TIMP-2 (bottom, orange). The N-terminus of MT1-MMP extends to the left, and the C-terminus of TIMP-2 to the bottom. Strands and helices are labelled, the six disulfide bridges of TIMP-2 are displayed in green, and the spheres represent the catalytic and structural zinc (central and upper pink sphere), and calcium 1 and 2 (right and left white sphere) of cdMT1-MMP. (**B**) Superposition of the complex formed between cdMT1-MMP (gold) and TIMP-2 (orange) with the complex (Gomis-Rüth *et al*., 1997) formed between cdMMP-3 (blue) and TIMP-1 (grey). Both MMP components superimpose well, while the two TIMP components are twisted to one another.

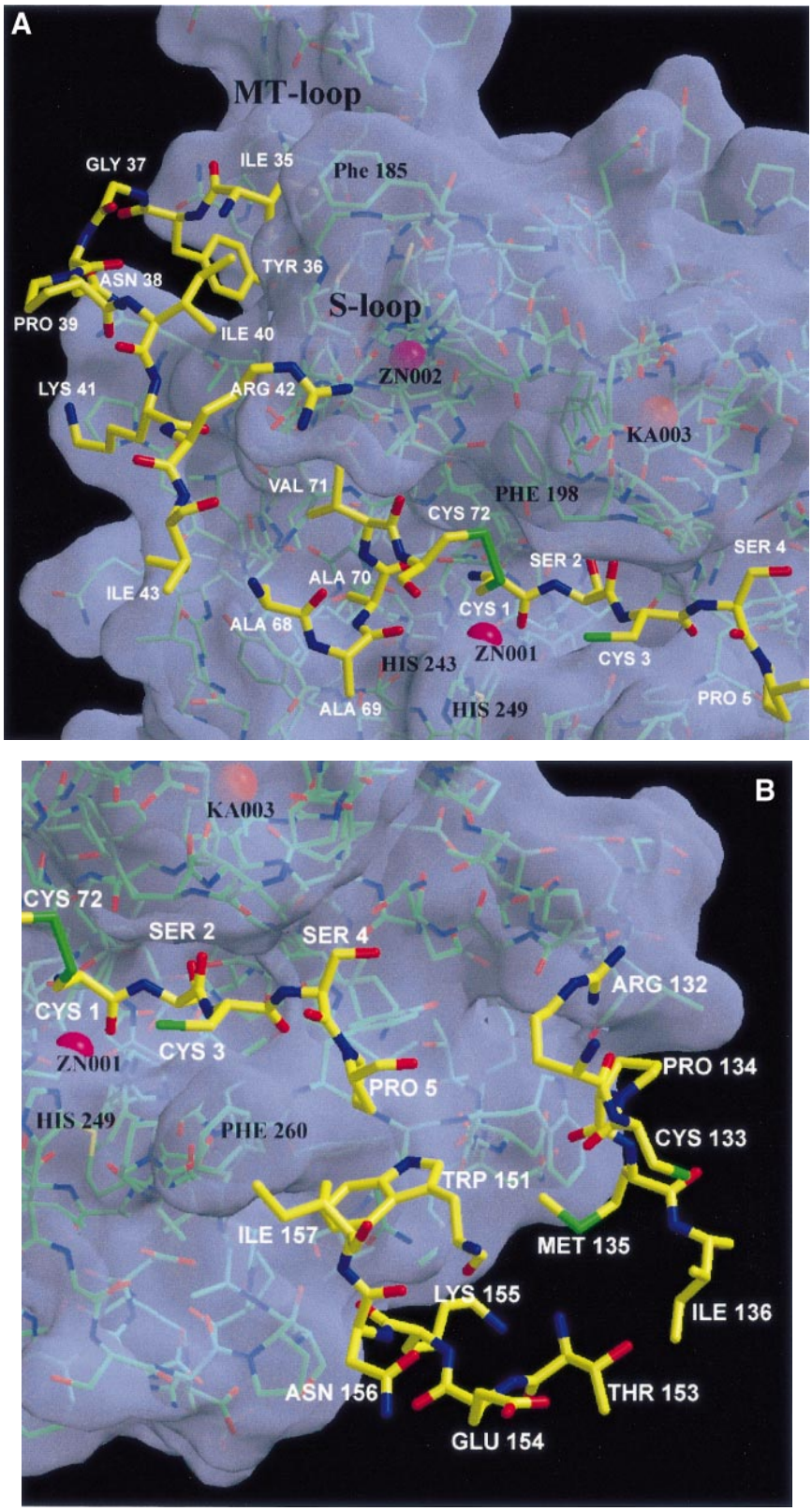

Fig. 2. Binding of the interacting edge segments of TIMP-2 (stick models with carbons in yellow, nitrogens in blue, oxygens in red, and sulphurs in green, labels in white) and the zinc (pink spheres) to the substrate binding region of MT1-MMP (green model, black labels), which is viewed through the half-transparent enzyme surface (blue). The catalytic (ZN001) and the structural zinc (ZN002), and one of both calcium ions (KA003) are shown as pink and red spheres, respectively. For the sake of simplicity, not all contacting segments are shown. This (standard orientation) view is achieved after an ~90° rotation of the complex in Figure 1 around a horizontal axis, so that now the active-site cleft runs across the MMP surface. Figures made by a combination of GRASP (Nicholls *et al*., 1993) and MOLSCRIPT (Kraulis, 1991). (**A**) Interaction of the sA–sB loop (represented by residues IleI35 to IleI43, left), the sC–connector loop (residues AlaI68 to CysI72, centre) and the N-terminal segment (CysI1 to ProI5, right) with the 'left side' part of the active-site cleft. (**B**) Interaction of the N-terminal segment (CysI1 to ProI5), the sG–sH loop (ArgI132 to IleI136) and the multiple turn loop (TrpI151, ThrI153 to IleI157) with the 'right side' part of the active-site cleft.

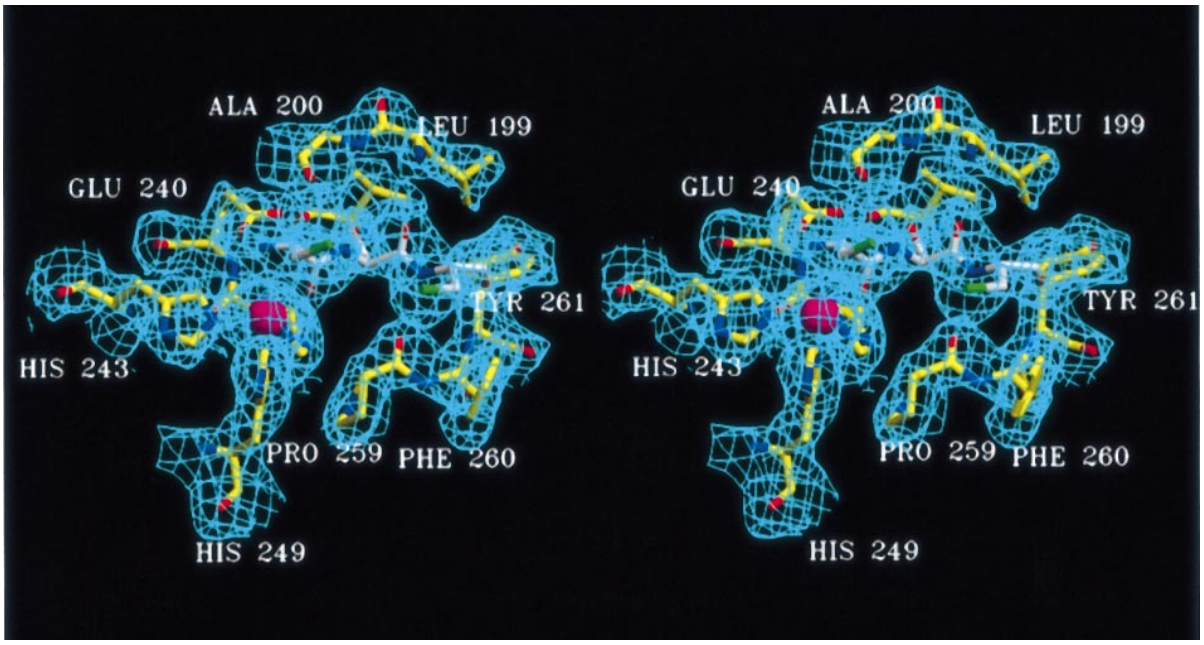

Fig. 3. Stereo 'standard' view of a section of the final 2.75 Å $2F_{obs}–F_{calc}$ electron density (blue net) around the catalytic zinc (pink sphere), superimposed with fragments of the final model. Carbon atoms of TIMP-2 and of MT1-MMP are given in white and yellow. TIMP segment CysI1-SerI2-CysI3 (centre, right) intercalates between the bulge segment (top, right) and the wall-forming segment (bottom, right) of MT1-MMP. The three imidazol side-chains of His239, 243 and 249 and Cys1I O and NH ligand the catalytic zinc. The catalytic Glu240 is on top. Figure produced with SETOR (Evans, 1993).

arranged in a slightly different conformation from that known of the classical MMPs. The C-terminal part of this S-shaped double loop encircles calcium ion KA003, while the second calcium, KA004, is bound between the bulged sIV-sV loop and sIII (Figure 1A).

The overall polypeptide fold of cdMT1-MMP is similar to that of the classical MMPs (Figure 1B), and both share virtually identical regular secondary structure elements (Figure 4). If 23 or 32 residues are omitted from a comparison with MMP-8 (Bode *et al*., 1994) and MMP-3 (Gomis-Rüth *et al*., 1997), the residual MT1-MMP C_α atoms show r.m.s. deviations of 0.72 and 0.71 Å, respectively. After the first three residues (Ile114 to Gly116) the N-terminal chain of cdMT1-MMP runs in a similar manner as in the classical MMPs. The most significant deviation occurs in the sII–sIII loop, which in MT1-MMP bridges over strand sI, and winds around the side chains of residue 127 (Cys in MT1-MMP) and Met178, but is considerably longer with 16 residues between Arg160 and Ile177 replacing eight equivalent residues in the classical MMPs. Most of the inserted residues of this 'MT-loop' characteristic for MT-MMPs (see Figure 4) are accommodated between Tyr164 and Gln174, where the chain bulges out into solution and is quite flexible due to lack of direct support by the molecular surface. The underlying thiol group of Cys127, which replaces an Arg residue in the classical MMPs but Ser residues in MT2- and MT3-MMP (Figure 4), is directed towards the Ala165 NH group, apparently stabilizing the MT-loop via a hydrogen bond. Between Trp221 and Gly230, the sV-hB connecting loop of cdMT1-MMP comprises eight residues compared with five or six in the classical MMPs (Figure 4), giving rise to a larger extension. The open loop, which connects the wall-forming segment with helix C, differs in MT1-MMP from that of MMP-3 (Figure 1B), but is similar to that of MMP-8 (Bode *et al*., 1994).

The TIMP-2 structure

The TIMP-2 molecule exhibits a wedge-like shape. It consists of an N-terminal segment (CysI1 to ValI6), an all-β-structure left-hand part (AspI16 to ThrI109), an all-helical centre (HisI7 to AlaI15, and SerI111 to CysI126), and a β-turn structure to the right (Figure 1A). Similar to TIMP-1, the TIMP-2 polypeptide chain forms with CysI1-SerI2-CysI3-SerI4 the central part of the inhibitor edge, turns towards the molecular centre and passes α-helix I, before it forms the five-stranded β-pleated sheet of Greek-key topology (comprising mostly antiparallel β-strands sA to sF, see Figures 1A and 5) rolled into a closed β-barrel of elliptical cross-section also called OB-fold (see Williamson *et al*., 1994; Gomis-Rüth *et al*., 1997). The narrower opening of this barrel is bounded by a multiple-turn segment, while its wider exit is bordered by an extended 'connector', which connects strands sC and sD.

After leaving strand sF, the polypeptide chain runs back to the centre, passes helices II and III, forms a β-strand-loop-parallel β-strand motive (sG...sH), participates in the edge region in a wide multiple-turn loop, and terminates in β-hairpin-sheet sI...sJ (Figure 1A). From AlaI181-AlaI182 onwards, the increasingly flexible TIMP-2 polypeptide chain leaves the molecular surface, with continuous electron density disappearing around ProI184 in the surrounding bulk water. The last 10 residues of TIMP-2 do not exhibit a defined conformation.

As in TIMP-1, the N-terminal CysI1-SerI4 segment is flanked by the sA–sB loop and the sC-connector loop on

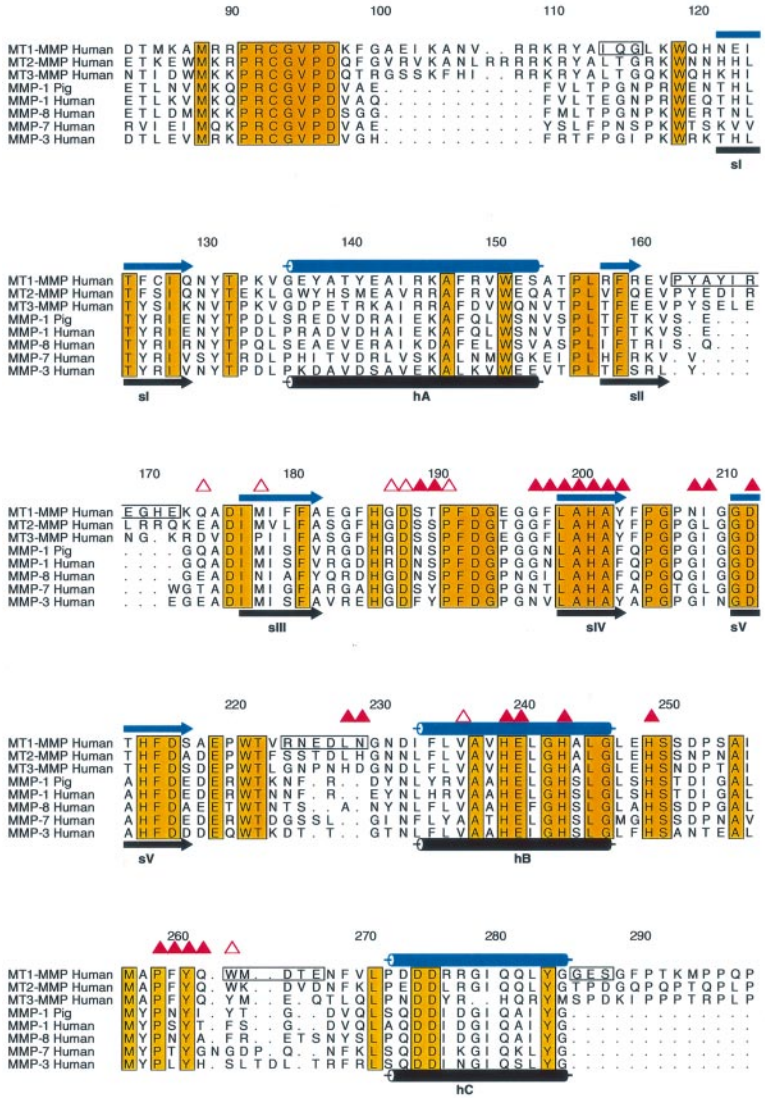

Fig. 4. Alignment of the catalytic domains of the MT1,2,3-MMPs (Okada *et al*., 1995; Takino *et al*., 1995; Will and Hinzmann, 1995) and MMPs 1, 3, 7 and 8 made according to topological equivalency. Strands (arrows) and helices (cylinders) are indicated for MT1-MMP (top) and MMP-3 (bottom), and residues strongly and weakly involved in sub 4.0 Å intermolecular atom–atom contacts are marked by filled and open triangles. Open boxes indicate segments of MT1-MMP strongly deviating from MMP-3, and strictly conserved residues are boxed in orange. The numbering is that of the naturally expressed MT1-MMP (Okada *et al*., 1995). Figure produced with ALSCRIPT (Barton, 1993).

the left-hand side, and by the sG–sH loop and the multiple turn loop on the right-hand side. These five segments together form the molecular edge, under some divergence of the pointed sA–sB hairpin (Figure 1A). The N-terminal strand is tightly connected to the neighbouring sC-connector loop and to the underlying E–F loop via disulfide bridges CysI1-CysI72 and CysI3-CysI101, respectively.

In spite of the 40% sequence identity (Figure 5), the topological congruence between TIMP-2 and TIMP-1 is considerably lower than that between MT1-MMP and MMP-3; optimal superposition requires omission of 60 residues, so that the residual 120 C_α atoms show an r.m.s. deviation of 1.1 Å upon optimal superposition. Particularly noteworthy are the much longer sA–sB loop and the twisted sG–sH loop at the edge side, the modified sD–sE loop in the molecular centre, and the less exposed sB–sC loop, the tipped up sI–sJ loop and the protruding C-terminus on the wedge side (see Figure 1B). The sA-sB β-hairpin loop of TIMP-2, elongated (compared with TIMP-1) between ValI29 and ArgI42 through the insertion of seven additional residues, does not follow the OB barrel surface curvature but is twisted and extends away. Its tip, made up of residues AspI34-IleI35-TyrI36-GlyI37, forms a 1,4 tight turn (Figure 2A). The partially disordered sG–sH loop of TIMP-2 is of similar overall conformation as in TIMP-1 (with ProI137 apparently *in cis* conformation) but somewhat rotated about its long axis, while the adjacent multiple-turn loop is better defined than that of TIMP-1 (Figure 1B). Remarkable is the novel 'pore' (not shown) of TIMP-2 left in the crook formed by the almost perpendicular N-terminal segments CysI1-SerI4 and ProI5-HisI7 and bounded by strand sF, created due to a considerable displacement of the ProI5-ValI6 segment compared with TIMP-1 (Figure 1B).

The cdMT1-MMP–TIMP-2 interface

As in the cdMMP-3–TIMP-1 complex, the TIMP-2 component interacts with its cognate cdMT1-MMP

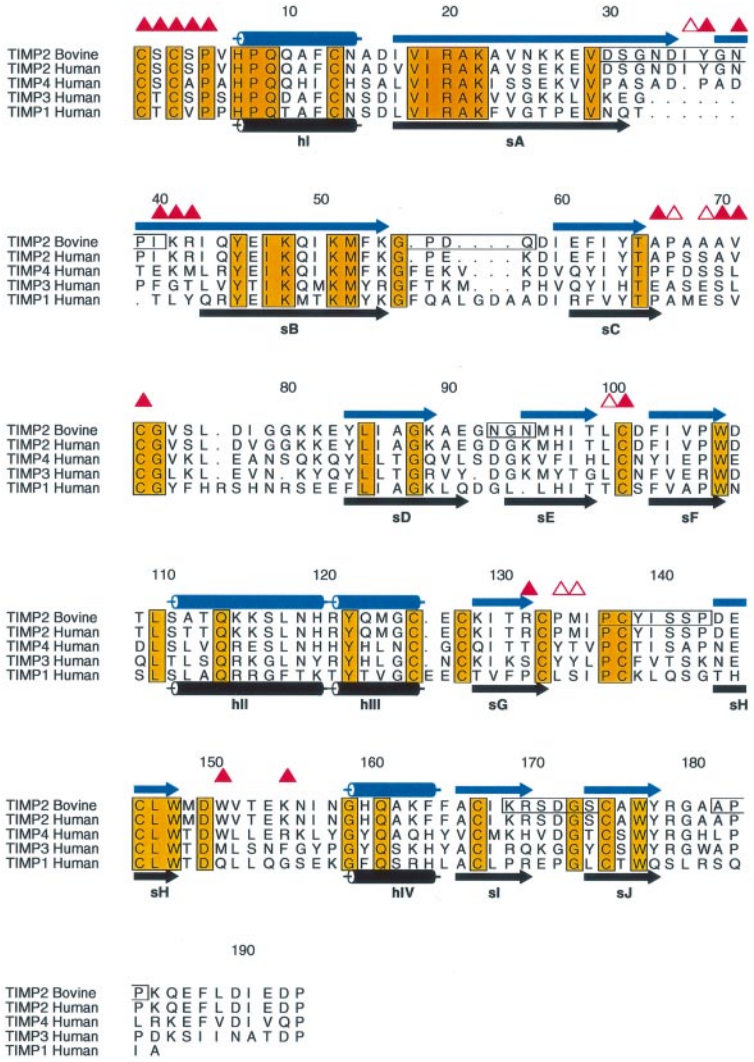

Fig. 5. Alignment of bovine (Boone *et al.*, 1990) and human TIMP-2 (Stetler-Stevenson *et al.*, 1989) with human TIMP-1 (Docherty *et al.*, 1985), 3 (Apte *et al.*, 1994) and 4 (Greene *et al.*, 1996) made according to (in part inferred) topological equivalency. Strands (arrows) and helices (cylinders) are indicated for TIMP-2 (top) and TIMP-1 (bottom), and residues strongly and weakly involved in sub 4.0 Å intermolecular atom–atom contacts are marked by filled and open triangles, respectively. Open boxes indicate segments of TIMP-2 strongly deviating from TIMP-1, and strictly conserved residues are boxed in orange. The numbering is that of the mature TIMP-2. Figure produced with ALSCRIPT (Barton, 1993).

through six sequentially separated segments (see Figures 4 and 5 for close contacts). Similar to the TIMP-1 complex, 97 (non-hydrogen) atom–atom contacts below 4.0 Å, i.e. 3/5 of all intermolecular contacts, are made by the N-terminal segment CysI1-ProI5, the sC–connector loop and the connecting disulfide bridge, while the sE–sF loop (nine contacts) and in particular the sA–sB loop (35 contacts) make more tight interactions (see Figure 2). The corresponding numbers of contacts for the C-terminal sG-sH loop (13 contacts) and the multiple-turn loop (12 contacts) are similar to MMP-3–TIMP-1; these latter two loops are better defined in cdMT1-MMP–TIMP-2, however.

The first five TIMP-2 residues CysI1 to ProI5 bind to the cdMT1-MMP active site similar to P1, P1′, P2′, P3′ and P4′ peptide substrate residues forming five inter-main-chain hydrogen bonds, while the AlaI70-ValI71 segment interacts in a somewhat substrate-inverse manner with subsites S2 and S3 (Figure 2). The AlaI68-ValI71 segment bulges into the enzyme, with AlaI70 Cβ poking against the Phe204 benzyl group and the ValI71 isopropyl group slotting into a hydrophobic groove formed by the enzyme side-chains of Tyr203 (sIV), His201 and the S-loop. CysI1 placed above the catalytic zinc provides its α-amino group and carbonyl oxygen as the fourth and fifth ligand to the catalytic zinc, with the α-amino group probably donating hydrogen bonds toward one carboxylate oxygen (Oε1) of the catalytic Glu240 (Figure 3) as well as to the carbonyl group of AlaI70. The SerI2 side chain of TIMP-2 is directed towards the large S1′ pocket of MT1-MMP, with the electron density indicating that its Oγ atom is hydrogen bonded to Oε2 of the catalytic Glu240. Although only one solvent molecule can be localized, the deep S1′ pocket (Figure 2A) must also accommodate some disordered solvent molecules. The side chain of the central residue of the wall-forming segment Phe260, which is conserved in MT-MMPs-14 to -16 (Figures 3 and 4), grasps around the N-terminal segment of TIMP-2 stoppering with its phenyl side chain the elbow pore of TIMP-2 mentioned above.

The long sA–sB hairpin loop of TIMP-2 folds over the rim of the active-site cleft and reaches up to the β-sheet of MT1-MMP. The exposed side-chain of TyrI36 slots into the surface gap left by the MT-loop, the side chains of Asp212 (sV) and Phe180 (sIII), and the S-loop of cdMT1-MMP (Figures 1A and 2A), making hydrogen bonds with the carboxylate oxygens of Asp212 besides a number of van der Waals contacts. With its ascending sA strand around IleI35 and the descending sB strand around IleI40, this loop touches the N-terminal part of MT1-MMP′s S-loop, under formation of a single inter-main-chain hydrogen bond and polar interactions through the ArgI42 side chain. In spite of the relatively large overall interface between the sA–sB loop and the MT1 surface, most of the distinct contacts do not seem designed for optimal complementarity. The same is true for the two edge loops provided by the C-terminal part of TIMP-2; the multiple-turn loop, in particular, nestles with the clustered side-chains of TrpI151 and IleI157 towards the wall-forming segment and the Phe260 benzyl group of MT1-MMP (Figure 2B). TrpI151 and IleI157 are conserved within the TIMP-2 species, but are replaced by Gln and Asp/Glu residues, respectively, in TIMP-1 (Figure 5).

Discussion

This analysis reveals that the cdMT1-MMP–TIMP-2 complex has an overall structure similar to the cdMMP-3–TIMP-1 complex solved previously. However, in spite of the relatively high sequence similarities to their respective protein relatives, each component exhibits unique features, and also the interaction interface displays remarkable differences.

Peculiar to the catalytic domain of MT1-MMP (and probably also of the other MT-MMPs) are conformation and length of the N-terminal segment, the characteristic MT-loop, and the sV–hB loop (see Figures 1A and 4). The N-terminus, in our cdMT1-MMP starting with Ile114, might be truncated compared with the naturally occurring MT1-MMP; in a furin-activated MT1-MMP species the N-terminal Tyr112-Ala113-Ile114 tripeptide (after rotation of Ile114 and displacement of the side chain of Glu248) could span the distance to the carboxylate group of Asp274 (the intermediate Asp in the Asp triple in hC, see Figure 4) to form a surface-located salt bridge, in a similar manner as made by Phe79-Met80-Leu81 in MMP-8 (Reinemer *et al*., 1994). An equivalent ‘superactivity’ of an adequately tailored MT-MMP remains to be shown experimentally, however. The exposed MT-loop replacing a short bridge in the classical MMPs projects away from the β-sheet surface, but does not extend into the active-site cleft. Larger protein substrates such as progelatinase A could certainly contact this loop; its conservation among the MT-MMPs underscores its possible importance as a secondary recognition exosite. The substrate binding region of MT1-MMP looks similar to that of the classical MMPs. Its voluminous S1′ pocket, much larger than needed for accommodation of a P1′-Ile/Leu side-chain as in MMP-3, is in agreement with the observed cleavage preference of MT1-MMP for peptide substrates with long bulky P1′-analogues compared with Leu (Mucha *et al*., 1998). As shown by its capability to cleave progelatinase A at the natural Asn-Leu but not at a mutated Ile-Val processing site (Kinoshita *et al*., 1996), MT1-MMP shares the unwillingness to cleave peptide bonds N-terminal of β-branched P1′ amino acids with the classical MMPs.

Particularly remarkable features of the bovine TIMP-2 component are the quite elongated twisted sA–sB hairpin loop and the negatively charged flexible C-terminal tail. With only 11 conservative residue exchanges (Figure 5), human TIMP-2 is likely to be virtually identical to the bovine molecule. TIMP-4, with 52% sequence identity, might share most of the characteristic topological elements with TIMP-2, and also seems to resemble it with respect to progelatinase A binding (Bigg *et al*., 1997). TIMP-3, in spite of a similar 50% sequence identity, exhibits a short sA–sB loop and a long but not negatively charged tail (see Figure 5); nevertheless, TIMP-3 is found to bind cdMT1-MMP with a similar association rate as TIMP-2 (Butler *et al*., 1997).

K_i-values in the (sub)nanomolar range have been communicated for different MT1-MMP–TIMP-2 complexes (Lichte *et al*., 1996; Olson *et al*., 1997; Zucker *et al*., 1998). Structure-based correlations of these K_i-values with the inhibitor loop–MMP subsite interactions will become possible only when the structures of the free components of the complex become available. According to NMR chemical shift data (Williamson *et al*., 1997), the N-terminal TIMP-2 segment, and in particular the long sA–sB loop of the isolated N-TIMP-2 molecule, are flexible relative to the main molecular body; presumably, this can also be assumed for both C-terminal edge loops in the full-length inhibitor. Upon complex formation, these edge loops become more rigid, with the sA–sB loop wrapping around the S-loop and snuggling up into the MT1-MMP surface fork. It is possible that the establishment of some of these apparently favourable intermolecular contacts might result in compromises at other interaction sites, as might be reflected by the overall tilt observed for the MT1-MMP–TIMP-2, relative to the MMP3–TIMP-1 complex. More detailed information will be available from the structures of the individual proteins and from designed mutants such as TIMP-2 variants having a truncated sA–sB loop. Interestingly, the formal numbers of intermolecular atom–atom contacts below 4.0 Å and the buried molecular surfaces are relatively similar for cdMT1-MMP–TIMP-2 and cdMMP-3–TIMP-1, in spite of the differences at the sA–sB loops. Indeed, the similar k_{on}-values of TIMP-3 (with a truncated sA–sB loop) with cdMT1-MMP (d’Ortho *et al*., 1997) show that the reduced amount of sA–sB contacts might be compensated for by more favourable contacts at other sites. Presumably, such a compensation is not possible for the interaction of TIMP-1 with MT1-MMP. A visual comparison of our crystal structures at least does not indicate serious obstacles that could easily explain the low affinity of TIMP-1 for MT1-MMP. The enormous influence of TIMP-1 residue 2 on the affinity for MMPs (Huang *et al*., 1997) nicely illustrates how single-site interactions can affect binding.

Our experimental cdMT1-MMP–TIMP-2 complex is furthermore of particular importance in that it represents the soluble part of the membrane receptor required for *in vivo* activation of progelatinase A. The catalytic MT1-MMP domain itself is able to catalyze this activation (Lichte *et al*., 1996), but seems to be effective only at high concentrations of the proenzyme (Will *et al*., 1996).

However, at low, i.e. presumably physiological proenzyme concentrations, an efficient activation seems to require the membrane-anchored MT1-MMP–TIMP-2 complex (Cao *et al*., 1995), which probably concentrates the progelatinase A in the vicinity of residual active MT1-MMP molecules (Butler *et al*., 1998).

The currently available structures, together with domain and single-site mapping results, allow an outline of this quarternary activation complex to be drawn. In this complex, the haemopexin-like domain of full-length MT1-MMP might be arranged to its catalytic domain in a similar manner as known for full-length porcine MMP-1 (Li *et al*., 1995; see also Gomis-Rüth *et al*., 1997), i.e. with TIMP-2, the catalytic and the haemopexin-like domain of MT1-MMP forming a triangular moiety, which as a whole might be kept close to the outer membrane surface via the trans-membrane segment of the complexed MT1-MMP. A full-length progelatinase A molecule could align to the TIMP-2 base, presumably through electrostatic interactions made between the negatively charged C-terminal tail of TIMP-2 and a positively charged surface patch of propeller blades III/IV including the Lys566, Lys567 and Lys568 cluster of the haemopexin-like domain of gelatinase A (Willenbrock *et al*., 1993; Kolkenbrock *et al*., 1994; Gohlke *et al*., 1996; Butler *et al*., 1998). In this way the prodomain of the bound progelatinase A molecule is presented to a second membrane-bound active MT1-MMP molecule in a manner suitable for partial cleavage; the gelatinase A intermediate thus produced could in turn be processed to the mature enzyme by autocatalytic activation cleavage, maybe through another membrane-bound gelatinase A molecule (Brooks *et al*., 1996).

Materials and methods

A DNA construct encoding the propeptide, the catalytic domain and the linker to the haemopexin-like domain of proMT1-MMP (Ala21-Ile318, using the cDNA numbering) was expressed as inclusion bodies in *Escherichia coli*. Upon refolding, the insoluble material yielded the autocatalytically processed catalytic domain cdMT1-MMP (Ile114-Ile318) as described previously (Lichte *et al*., 1996). Bovine TIMP-2 (CysI1-ProI194) was isolated from BSP and purified as recently described (Calvete *et al*., 1996). The cdMT1-MMP–TIMP-2 complex was formed by mixing equimolar amounts of both components for 2 h in 500 mM NaCl, 5 mM $CaCl_2$, 0.1 mM $ZnCl_2$, and 20 mM Tris–HCl pH 7.5, and further purified by gel filtration on a Sephadex S-100 column equilibrated with the incubation buffer.

The cdMT1-MMP–TIMP-2 complex was crystallized at a concentration of 10 mg/ml at room temperature in ~20 mM $BaCl_2$, 10 mM $MgCl_2$, 5 mM $CaCl_2$, 100 mM NaCl, 100 mM $(NH_4)_2SO_4$, 16% w/v PEG 8000, and MES/NaOH at pH 5.6 using the vapour diffusion technique. The plate-like crystals belong to the monoclinic space group C2, and have cell constants a = 102.65 Å, b = 40.10 Å, c = 85.68 Å, β = 102.3°, and contain one complex per asymmetric unit. Initially, these crystals diffract to beyond 2.5 Å resolution.

A complete X-ray data set to 2.5 Å (Table I) was collected from one single crystal mounted together with its mother liquor in a capillary on a MAR Research 300 image plate detector at room temperature using monochromatized CuKα radiation produced by a conventional rotation anode. 73215 reflections were evaluated, merged and scaled with DENZO (Otwinowski and Minor, 1993) yielding 11911 unique reflections to 2.5 Å resolution (Table I). The structure of the complex was solved by molecular replacement with AMoRe (Navaza, 1994) by independently searching for the orientation and position of the separate components of the complex using modified models of cdMMP-3 and TIMP-1 of our cdMMP-3–TIMP-1 structure (Gomis-Rüth *et al*., 1997). After several unsuccessful attempts, the search yielded one outstanding solution (correlation factor 37.5%, R-factor 45.6% at 3.5 Å). The placement of both components of the initial model was further optimized by one round of rigid body refinement with X-PLOR (Brünger, 1992), followed by energy-restrained positional refinement. The model was completed in several cycles consisting of electron density calculation, (re)modelling on an SGI graphics workstation using TurboFRODO (Roussel and Cambilleau, 1989), and restrained crystallographic refinement including slow-cooling using X-PLOR (Brünger, 1991) and REFMAC (CCP4, 1994). In the course of refinement, the data were gradually extended to 2.75 Å (thus omitting the outermost data to 2.5 Å, which did not improve the quality of the Fouriers, see Table I). At an *R* value of 30%, 'kick-omit' maps calculated and visualized with MAIN (Turk, 1992) helped to trace some badly defined segments. Most solvent molecules interpreted as waters were placed at sites showing high electron density (1σ) and difference density values (2σ) if close to polar protein or solvent groups; in addition, a few density strings extending into the solvent cavities and probably accounting for the C-terminal extensions of both components were filled with a number of non-contacting water molecules. At the end, also individual temperature factors were refined with REFMAC employing strong bonded-atom B-factor restraints.

Table I. X-ray data and refinement statistics

Crystals cell constants a = 102.65 Å, b = 40.10 Å, c = 85.68 Å, β = 102.3°	
Space group monoclinic	C 2
Limiting resolution (Å)	2.5
Reflections measured	73215
Reflections unique (25.0–2.5 Å)	11911
R_{merge} (%)[a], overall	9.5
R_{merge} (%)[a], (2.6–2.5 Å)	38.9
Completeness (%), overall (Å)	97.0
Completeness (%), (2.6–2.5 Å)	93.2
Non-hydrogen protein atoms	2835
Solvent molecules	317
Zinc ions	2
Calcium ions	2
Reflections used for refinement	8537
Resolution range (Å)	8.0–2.75
R value (%)[b], overall	18.9
R_{free} (%)[c], from 7% of the data	24.8
r.m.s standard deviations:	
bond length (Å)	0.018
bond angles (degrees)	1.88
average B-value/SD[3] (Å^2)	3.0

[a]$R_{merge} = [\Sigma_h\Sigma_i |I(h,i)-<I(h)>|/\Sigma_h\Sigma_i I(h,i)]\times 100$.
[b]*R* value $= (\Sigma| F_{obs}-F_{calc} |/\Sigma F_{obs})\times 100$.
[c]Standard deviation is from bonded atoms.

The final model consists of segments Ile114-Ser287 (cdMT1-MMP), CysI1-ProI184 (TIMP-2), 317 water molecules, and two zinc and two calcium ions (Table I). Short breaks in the continuous electron density accounting for the polypeptide main chains occur in the cdMT1-MMP structure at Arg148 (MT-loop), and in the TIMP-2 structure at ThrI78 (Connector-D loop) and SerI142 (sG–sH). The final R-factor is 18.9%, and the R_{free} determined by random selection of 7% of the data is 24.8%. All main-chain angles of non-glycine residues fall into the conformationally most favoured and allowed regions of the Ramachandran plot (Laskowski *et al*., 1993). The r.m.s. deviations from target values (Engh and Huber, 1991) of all protein bond lengths and angles are 0.018 Å and 1.9 °. The coordinates will be deposited at the Protein Data Bank and released one year after publication.

Acknowledgements

We thank M.Braun for her excellent help with crystallization, Drs F.H.Büttner and E.Bartnik (HMR, Wiesbaden) for providing the full-length cDNA of MT1-MMP, Dr A.Bergner for help with the figures, and Dr M.T.Stubbs for valuable discussions. The financial support by the SFB469, by the Biotechnology Program (contract ERBBIO4-CT960464) of the European Union, by the Fonds der Chemischen Industrie (W.B.), and by the SFB223 and 549 (H.T.) is kindly acknowledged.

References

Apte,S.S., Olsen,B.R. and Murphy,G. (1995) The gene structure of tissue inhibitor of metalloproteinases (TIMP)-3 and its inhibitory activities define the distinct TIMP gene family. *J. Biol. Chem.*, **270**, 14313–14318.

Barton,G.J. (1993) ALSCRIPT: a tool to format multiple sequence alignments. *Protein Eng.*, **6**, 37–40.

Bigg,H.F., Shi,Y.E., Liu,Y.E., Steffensen,B. and Overall,C.M. (1997) Specific, high affinity binding of tissue inhibitor of metalloproteinases-4 (TIMP-4) to the COOH-terminal hemopexin-like domain of human gelatinase A. *J. Biol. Chem.*, **272**, 15496–15500.

Bode,W., Reinemer,P., Huber,R., Kleine,T., Schnierer,S. and Tschesche,H. (1994) The X-ray crystal structure of the catalytic domain of human neutrophil collagenase inhibited by a substrate analogue reveals the essentials for catalysis and specificity. *EMBO J.*, **13**, 1263–1269.

Boone,T.C., Johnson,M.J., De Cle,Y.A. and Langley,K.E. (1990) cDNA cloning and expression of a metalloproteinase inhibitor related to tissue inhibitor of metalloproteinases. *Proc. Natl Acad. Sci. USA*, **87**, 2800–2804.

Brooks,P.C., Strömblad,S., Sanders,L.C., vonSchalscha,T.L., Aimes,R.T., Stetler-Stevenson,W.G., Quigley,J.P. and Cheresh,D.A. (1996) Localization of matrix metalloproteinase MMP-2 to the surface of invasive cells by interaction with integrin αvβ3. *Cell*, **85**, 683–693.

Brünger,A.T. (1991) Simulated annealing in crystallography. *Annu. Rev. Phys. Chem.*, **42**, 197–223.

Brünger,A.T. (1992) *X-PLOR Version 3.1 A System for X-Ray Crystallography and NMR*. Yale University Press, New Haven, CT.

Butler,G.S., Will,H., Atkinson,S.J. and Murphy,G. (1997) Membrane-type-2 matrix metalloproteinase can initiate the processing of progelatinase A and is regulated by the tissue inhibitors of metalloproteinases. *Eur. J. Biochem.*, **244**, 653–657.

Butler,G.S., Butler,M.J., Atkinson,S.J., Will,H., Tamura,T., van Westrum,S.S., Crabbe,T., Clements,J., d'Ortho,M.P. and Murphy,G. (1998) The TIMP2 membrane type 1 metalloproteinase 'receptor' regulates the concentration and efficient activation of progelatinase A. *J. Biol. Chem.*, **273**, 871–880.

Calvete,J.J., Varela,P.F., Sanz,L., Romero,A., Mann,K. and Töpfer-Petersen,E. (1996) A procedure for the large-scale isolation of major bovine seminal plasma proteins. *Protein Expr. Purif.*, **8**, 48–56.

Cao,J., Sato,H., Takino,T. and Seiki,M. (1995) The C-terminal region of membrane type matrix metalloproteinase is a functional transmembrane domain required for progelatinase A activation. *J. Biol. Chem.*, **270**, 801–805.

Cawston,T. (1998) Matrix metalloproteinases and TIMPs: properties and implications for the rheumatic diseases. *Mol. Med. Today*, **4**, 130–137.

Collaborative Computational Project, Number 4 (1994) The CCP4 suite: programs for protein crystallography. *Acta Crystallogr. D*, **50**, 760–763.

Docherty,A.J.P., Lyons,A., Smith,B.J., Wright,E.M., Stephens,P.E., Harris,T.J.R., Murphy,G. and Reynolds,J.J. (1985) Sequence of human tissue inhibitor of metalloproteinases and its identity to erythroid potentiating activity. *Nature*, **318**, 65–69.

Engh,R.A. and Huber,R. (1991) Accurate bond and angle parameters for X-ray protein structure refinement. *Acta Crystallogr. A*, **47**, 392–400.

Evans,S.V. (1993) SETOR: hardware lighted three-dimensional solid model representations of macromolecules. *J. Mol. Graph.*, **11**, 134–138.

Fridman,R., Fuerst,T.R., Bird,R.E., Hoyhtya,M., Oelkuct,M., Kraus,S., Komarek,D., Liotta,L.A., Berman,M.L. and Stetler-Stevenson,W.G. (1992) Domain structure of human 72-kDa gelatinase/typeIV collagenase. *J. Biol. Chem.*, **267**, 15398–15405.

Gohlke,U., Gomis-Rüth,F.-X., Crabbe,T., Murphy,G., Docherty,A.J.P. and Bode,W. (1996) The C-terminal (haemopexin-like) domain structure of human gelatinase A (MMP2): structural implications for its function. *FEBS Lett.*, **378**, 126–130.

Gomez,D.E., Alonso,D.F., Yoshiji,H. and Thorgeirsson,U.P. (1997) Tissue inhibitors of metalloproteinases: structure, regulation and biological functions. *Eur. J. Cell Biol.*, **74**, 111–122.

Gomis-Rüth,F.X. *et al.* (1997) Mechanism of inhibition of the human matrix metalloproteinase stromelysin-1 by TIMP-1. *Nature*, **389**, 77–81.

Green,J., Wang,M., Liu,Y.E., Raymond,L.A., Rosen,C. and Shi,Y.E. (1996) Molecular cloning and characterisation of human tissue inhibitor of metalloproteinase 4. *J. Biol. Chem.*, **271**, 30375–30380.

Huang,W., Meng,Q., Suzuki,K., Nagase,H. and Brew,K. (1997) Mutational study of the amino-terminal domain of human tissue inhibitor of metalloproteinases 1 (TIMP-1) locates an inhibitory region for matrix metalloproteinases. *J. Biol. Chem.*, **272**, 22086–22091.

Kinoshita,T., Sato,H., Takino,T., Itoh,M., Akizawa,T. and Seiki,M. (1996) Processing of a precursor of 72-kilodalton type IV collagenase/gelatinase A by a recombinant membrane-type 1 matrix metalloproteinase. *Cancer Res.*, **56**, 2535–2538.

Kolkenbrock,H., Orgel,D., Hecker-Kia,A., Noack,W. and Ulbrich,N. (1991) The complex between a tissue inhibitor of metalloproteinases (TIMP-2) and 72-kDa progelatinase is a metalloproteinase inhibitor. *Eur. J. Biochem.*, **198**, 775–781.

Kolkenbrock,H., Hecker-Kia,A., Orgel,D., Ruppitsch,W. and Ulbrich,N. (1994) Activity of ternary gelatinase A-TIMP-2-matrix metalloproteinase complexes. *Biol. Chem. Hoppe-Seyler*, **375**, 241–247.

Kraulis,P.J. (1991) MOLSCRIPT: a program to produce both detailed and schematic plots of proteins. *J. Appl. Crystallogr.*, **24**, 946–950.

Laskowski,R.A., MacArthur,M.W., Moss,D.S. and Thornton,J.M. (1993) PROCHECK: a programme to check the stereochemical quality of protein structures. *J. Appl. Crystallogr.*, **26**, 283–291.

Li,J.-Y. *et al.* (1995) Structure of full-length porcine synovial collagenase reveals a C-terminal domain containing a calcium-linked, four-bladed beta-propeller. *Structure*, **3**, 541–549.

Lichte,A., Kolkenbrock,H. and Tschesche,H. (1996) The recombinant catalytic domain of membrane-type matrix metalloproteinase-1 (MT1-MMP) induces activation of progelatinase A and progelatinase A complexed with TIMP-2. *FEBS Lett.*, **397**, 277–282.

Mucha,A., Cunisse,P., Kannan,R., Beau,F., Yiotakis,A., Basset,P. and Dive,V. (1998) Membrane type-1 matrix metalloprotease and stromelysin-3 cleave more efficiently synthetic substrates containing unusual amino acids in their P1′ positions. *J. Biol. Chem.*, **273**, 2763–2768.

Murphy,G. and Willenbrock,F. (1995) Tissue inhibitors of matrix metalloendopeptidases. *Methods Enzymol.*, **248**, 496–510.

Murphy,G., Willenbrock,F., Ward R.V., Cockett,M.I., Eaton,D. and Docherty,A.J.P. (1992) The C-terminal domain of 72 kDa gelatinase A is not required for catalysis, but is essential for membrane activation and modulates interactions with tissue inhibitors of metalloproteinases. *Biochem. J.*, **283**, 637–641.

Nagase,H. (1997) Activation mechanisms of matrix metalloproteinases. *Biol. Chem.*, **378**, 151–160.

Navaza,J. (1994) AMoRe: an automated package for molecular replacement. *Acta Crystallogr. Sect* **A 50**, 157–163.

Nicholls,A., Bharadwaj,R. and Honig,B. (1993) Grasp—graphical representation and analysis of surface properties. *Biophys. J.*, **64**, A166.

Ohuchi,E., Imai,K., Fujii,Y., Sato,H., Seiki,M. and Okada,Y. (1997) Membrane type 1 matrix metalloproteinase digests interstitial collagens and other extracellular matrix macromolecules. *J. Biol. Chem.*, **272**, 2446–2451.

Okada,A., Bellocq,J.-P., Rouyer,N., Chenard,M.-P., Rio,M.-C., Chambon,P. and Basset,P. (1995) Membrane-type matrix metalloproteinase (MT-MMP) gene is expressed in stromal cells of human colon, breast and head and neck carcinomas. *Proc. Natl Acad. Sci. USA*, **92**, 2730–2734.

Olson,M.W., Gervasi,D.C., Mobasheri,S. and Fridman,R. (1997) Kinetic analysis of the binding of human matrix metalloproteinase-2 and -9 to tissue inhibitor of metalloproteinase (TIMP)-1 and TIMP-2. *J. Biol. Chem.*, **272**, 29975–29983.

d'Ortho,M.-P., Will,H., Atkinson,S., Butler,G., Messent,A., Gavrilovic,J., Smith,B., Timpl,R., Zardi,L. and Murphy,G. (1997) Membrane-type matrix metalloproteinases 1 and 2 exhibit broad-spectrum proteolytic capacities comparable to many matrix metalloproteinases. *Eur. J. Biochem.*, **250**, 751–757.

Otwinowski,Z. and Minor,W. (1993) *DENZO: A Film Processing for Macromolecular Crystallography*. Yale University, New Haven, CT.

Pei,D. and Weiss,S.J. (1996) Transmembrane-deletion mutants of the membrane-type matrix metalloproteinase-1 process progelatinase A and express intrinsic matrix-degrading activity. *J. Biol. Chem.*, **271**, 9135–9140.

Reinemer,P., Grams,F., Huber,R., Kleine,T., Schnierer,S., Pieper,M., Tschesche,H. and Bode,W. (1994) Structural implications for the role of the N-terminus in the 'superactivation' of collagenases—a crystallographic study. *FEBS Lett.*, **338**, 227–233.

Roussel,A. and Cambilleau,C. (1989) Turbo-Frodo in Silicon Graphics Geometry, Partners Directory, Silicon Graphics, Mountain View, CA.

Sato,H., Takino,T., Okada,Y., Cao,J., Shinagawa,A., Yamamoto,E. and Seiki,M. (1994) A matrix metalloproteinase expressed on the surface of invasive tumour cells. *Nature*, **370**, 61–65.

Sato,H., Kinoshita,T., Takino,T., Nakayama,K. and Seiki,M. (1996) Activation of a recombinant membrane type 1-matrix metalloproteinase (MT1-MMP) by furin and its interaction with tissue inhibitor of metalloproteinases (TIMP)-2. *FEBS Lett*., **393**, 101–104.

Stetler-Stevenson,W.G., Krutzsch,H.C. and Liotta,L.A. (1989) Tissue inhibitor of metalloproteinase (TIMP-2). *J. Biol. Chem*., **264**, 17374–17378.

Strongin,A.Y., Marmer,B.L., Grant,G.A. and Goldberg,G.I. (1993) Plasma membrane-dependent activation of the 72-kDa type IV collagenase is prevented by complex formation with TIMP-2. *J. Biol. Chem*., **268**, 14033–14039.

Strongin,A.Y., Collier,I.E., Bannikov,U., Marmer,B.L., Grant,G.A. and Goldberg,G.I. (1995) Mechanism of cell surface activation of 72-kDa type IV collagenase. *J. Biol. Chem*., **270**, 5331–5338.

Takino,T., Sato,H., Shinagawa,A. and Seiki,M. (1995) Identification of the second membrane-type matrix metalloproteinase (MT-MMP-2) gene from a human placenta cDNA library. *J. Biol. Chem*., **270**, 23013–23020.

Turk,D. (1992) Dissertation, TU München.

Will,H. and Hinzmann,B. (1995) cDNA sequence and mRNA tissue distribution of a novel human MMP with a transmembrane segment. *Eur. J. Biochem*., **231**, 602–608.

Will,H., Atkinson,S.J., Butler,G.S., Smyth,B. and Murphy,G. (1996) The soluble catalytic domain of membrane type 1 matrix metalloproteinase cleaves the propeptide of progelatinase A and initiates autocatalytic activation. *J. Biol. Chem*., **271**, 17119–17123.

Willenbrock,F., Crabbe,T., Slowcombe,M.P., Sutton,C.W., Docherty, A.J.P., Cockett,M.I., O'Shea,M., Brocklehurst,K., Phillips,I.R. and Murphy,G. (1993) The activity of the tissue inhibitors of metalloproteinases is regulated by C-terminal domain interactions: a kinetic analysis of the inhibition of gelatinase A. *Biochemistry*, **32**, 4330–4337.

Williamson,R.A., Martorell,G., Carr,M.D., Murphy,G., Docherty,A.J., Freedman,R.B. and Feeney,J. (1994) Solution structure of the active domain of tissue inhibitor of metalloproteinases-2. A new member of the OB fold protein family. *Biochemistry*, **33**, 11745–11759.

Williamson,R.A., Carr,M.D., Frenkiel,T.A., Feeney,J. and Freedman,R.B. (1997) Mapping the binding site for matrix metalloproteinase on the N-terminal domain of the tissue inhibitor of metalloproteinases-2 by NMR chemical shift perturbation. *Biochemistry*, **36**, 13882–13889.

Woessner,J.F., Jr (1991) Matrix metalloproteinases and their inhibitors in connective tissue remodeling. *FASEB J*., **5**, 2145–2155.

Zucker,S., Drews,M., Conner,C., Foda,H.D., DeClerck,Y.A., Langley, K.E., Bahou,W.F., Docherty,A.J.P. and Cao,J. (1998) Tissue inhibitor of metalloproteinase-2 (TIMP-2) binds to the catalytic domain of the cell surface receptor, membrane type 1-matrix metalloproteinase 1 (MT1-MMP). *J. Biol. Chem*., **273**, 1216–1222.

Received May 13, 1998; revised and accepted July 7, 1998